PHYSOR 2014 – The Role of Reactor Physics Toward a Sustainable Future
The Westin Miyako, Kyoto, Japan, September 28 – October 3, 2014, on CD-ROM (2014)

BIAS AND UNCERTAINTY ASSESSMENT OF PRESSURIZED WATER REACTOR FUEL ISOTOPICS USING SCALE

Ryan N. Bratton, Kostadin N. Ivanov
Department of Mechanical and Nuclear Engineering
The Pennsylvania State University, Pennsylvania, USA
rnb145@psu.edu
kni1@engr.psu.edu

Matthew A. Jessee, William A. Wieselquist
Reactor and Nuclear Systems Division
Oak Ridge National Laboratory, Tennessee, USA
jesseema@ornl.gov
wieselquiswa@ornl.gov

ABSTRACT

The purpose of this study is to investigate bias and uncertainty in fuel isotopic calculations for a well-defined radiochemical assay benchmark with Sampler, the new sampling-based uncertainty quantification tool in the SCALE code system. Isotopic predictions are compared to measurements of fuel rod MKP109 of assembly D047 from the Calvert Cliffs Unit 1 core at three axial locations, representing a range of discharged fuel burnups. A methodology is developed which quantifies the significance of input parameter uncertainties and modeling decisions on isotopic prediction by comparing to isotopic measurement uncertainties. The SCALE Sampler model of the D047 assembly incorporates input parameter uncertainties for key input data such as multigroup cross sections, decay constants, fission product yields, the cladding thickness, and the power history for fuel rod MKP109. The effects of each set of input parameter uncertainty on the uncertainty of isotopic predictions have been quantified. In this work, isotopic prediction biases are identified and an investigation into their sources is proposed; namely, biases have been identified for certain plutonium, europium, and gadolinium isotopes for all three axial locations. Moreover, isotopic prediction uncertainty resulting from only nuclear data is found to be greatest for Eu-154, Gd-154, and Gd-160.

Key Words: **SCALE, Sampler, uncertainty, bias, Calvert Cliffs, spent fuel isotopics**

1. INTRODUCTION

The quantification of model prediction bias and uncertainty due to input data uncertainty or modeling decisions is an important component of reactor modeling and simulation. However, in practice, model performance analyses frequently consider only experimental errors, with minimal evaluation of uncertainties associated with the calculations (beyond stochastic uncertainties in Monte Carlo simulations) due to the complexity of the task. Moreover, the identification of the sources of bias and uncertainty are essential to determine where additional efforts should be made to improve model predictions. In this work, the SCALE code system [1] is employed to quantify the bias and uncertainty in spent fuel isotopic calculations for a well-defined radiochemical assay (RCA) benchmark and to identify their respective sources.

New for the beta release of SCALE 6.2, the SCALE Sampler module provides uncertainty analysis for any multigroup SCALE calculation using stochastic sampling of the specified input parameters' uncertainties [2] and the uncertainties associated with the nuclear data used in the calculations. In this work, SCALE Sampler is used in conjunction with the two-dimensional (2-D) transport and depletion module, TRITON/NEWT [3], to model fuel assemblies from Calvert Cliffs Unit 1 (CC-1) PWR system designed by Combustion Engineering Co. This reactor system was chosen because detailed operating history information and isotopic measurements are available for fuel rod MKP109 of the discharged fuel assembly D047 [4]. Performing an input data uncertainty analysis on a well-documented reactor system such as CC-1 provides a means to determine biases in SCALE isotopic predictions. The cross-section, decay constant, and fission product yield data utilized in this study are based on the ENDF/B-VII.0 nuclear data files.

In this paper, the following definitions and notations are applied:

- **Bias (B)** – The relative difference between a calculated output (C) and a measured output (E), i.e., B = (C – E)/E. For bias assessments, the high- and low-fidelity calculated outputs are denoted E and C, respectively.
- **Standard Deviation** – Denoted SD(X) for variable X.
- **Covariance Matrix** – Denoted **C**(X) for vector X.
- **Bias Uncertainty** – The standard deviation in the bias, i.e., SD(B). Using the propagation of error formula,

$$SD(B) = \frac{1}{E}\sqrt{SD(C)^2 + \frac{C^2}{E^2}SD(E)^2}.$$

- **Chi-Squared** – Denoted χ^2. Formally, χ^2 is equal to $B^T\mathbf{C}(B)^{-1}B$. If the bias covariance matrix **C**(B) is diagonal, χ^2 is equal to sum of the squares of the bias of each output, inversely weighted by the standard deviation of the bias of each output.
- **Reduced Chi-squared** – χ^2 divided by the number of outputs.
- **Modeling-based Bias Assessment (MBA)** – Procedure described below to quantify the significance of modeling decisions on the bias.
- **Input-based Bias Assessment (IBA)** – Procedure described below to quantify the significance of model input uncertainties on the bias.
- **Input-based Uncertainty Quantification (IUQ)** – The quantification of calculated output uncertainty, i.e., mean, standard deviation, correlation coefficients, due to input parameter uncertainties. Uncertainty Quantification (UQ) is performed using SCALE Sampler via stochastic sampling techniques.

2. ASSEMBLY MODEL

Experimental data for assembly D047 of CC-1 is available in the literature [4]. The assembly is a Combustion Engineering (CE) design and consists of 176 fuel rods and five large water-filled rods. Assembly D047 was present in the CC-1 core for four irradiation cycles (Cycles 2–5) with no burnable absorbers or gadolinium-bearing fuel rods. Detailed measurement and operating data were provided for fuel rod MKP109 of this assembly such as local linear power rates and cumulative burnups. MKP109 is comprised of uranium oxide fuel, and its location in assembly D047

is displayed in Figure 1 as the blue fuel pin.

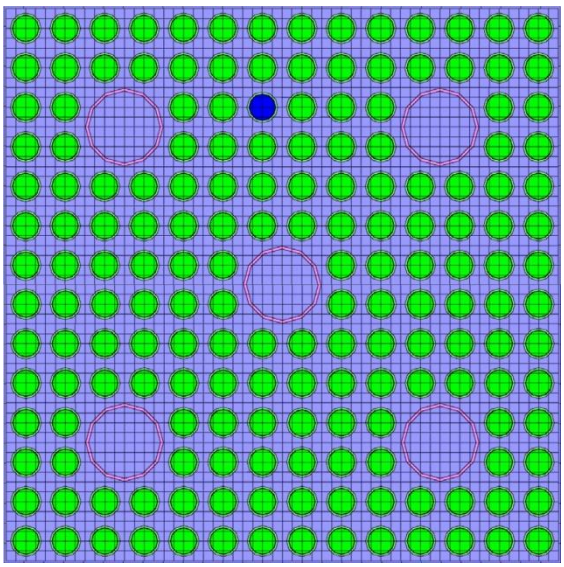

Figure 1. Assembly layout for assembly D047 and fuel pin MKP109 location.

Fuel rod MKP109 was destructively analyzed at three axial locations: 13.20, 27.70, and 165.22 cm from the bottom of the active fuel region. The end of cycle (EOC) and end of life (EOL) burnups for each axial location are summarized in Table 1 in GWd/MTU. Measurements were initially performed by Pacific Northwest National Laboratory (PNNL) in 1987 on the major actinides, neodymium, and several fission products. Measurements were later performed by Khlopin Radium Institute (KRI) in 1993 and 1995 on several lanthanides, such as the isotopes of neodymium, samarium, europium, and gadolinium [5].

Table 1. EOC and EOL burnups (GWd/MTU) for each axial location of fuel rod MKP109 [4].

Axial Location (cm)	Cycle 2	Cycle 3	Cycle 4	Cycle 5	EOL*
13.20	5.28	7.41	7.94	6.72	27.35
27.70	7.56	10.22	10.64	8.70	37.12
165.22	9.52	12.41	12.21	10.20	44.34

*Inferred values from neodymium measurements

Although numerous isotopic concentrations were measured by PNNL and KRI, not all concentrations were reported with uncertainty in those measurements. Furthermore, some isotopic measurements with uncertainties were not recommended for code validation purposes due to likely experimental errors [5]. Due to these factors, not all isotopes for which experimental data are available will be used. The isotopic measurements and their associated uncertainties are provided in Appendix A for convenience. Due to the fact that each laboratory performed its measurements at different times, the cooling time of the spent fuel should be accounted for in SCALE isotopic predictions. For all PNNL measurements, the cooling time is 1870 days. For the KRI

measurements, a cooling time of 4171 days applies for measurements of the 13.20 cm axial location and 4656 days for measurements of the 27.70 cm and 165.22 cm axial locations [5].

2.1. Bias Assessment Procedure

The SCALE Sampler calculation determines the uncertainty in calculated output parameters which may include potential biases due to modeling decisions made before simulation, i.e., approximations or simplifications required to simulate the model with reasonable computational resources and run-times. To quantify the bias due to modeling decisions, isotopic predictions were compared for a high-fidelity model and a low-fidelity model. In this approach, the bias is quantified as the relative difference between the high-fidelity model prediction (E) and the low-fidelity model prediction (C). The incorporation of the RCA measurement uncertainties onto the high-fidelity model provides a means to quantify the impact of the modeling decision, with respect to the measured isotope uncertainties. If the bias in an isotope prediction is small, e.g., less than 0.1 measured standard deviations, then the modeling decision does not introduce a significance bias. Conversely, if the bias is large, e.g., greater than 0.1 measured standard deviations, the modeling decision introduces a significant bias, and measures should be taken to reduce or account for this bias, namely a) reverse the modeling decision or b) utilize a bias factor correction [6] if applicable. At a minimum, identification of modeling decisions that introduce significant bias should be highlighted in the interpretation of input-based uncertainty quantification results.

In this work, a significant bias due to a modeling decision is said to exist if the reduced chi-squared exceeds 0.01, in other words, when the root mean square (RMS) of the isotope prediction relative differences between the high- and low- fidelity models ($\tilde{\Delta}_{m,i}$)—inversely weighted by the RCA isotopic measurement relative standard deviations ($\tilde{\sigma}_{m,i}$)— exceeds 0.1. This condition is synonymous with stating that if the difference between the two isotopic predictions is greater than 10% of a measurement standard deviation, then the difference is significant. In order to quantify this difference as a single value for the model comparison, the RMS of the values is appropriate. Explicitly, a bias is described as significant when the following expression is true:

$$0.1 < RMS\left(\frac{\tilde{\Delta}_{m,i}}{\tilde{\sigma}_{m,i}}\right).$$

The modeling-based bias assessment procedure described above can also be used to determine the impact of model input uncertainties on the calculation bias. Although several sources of model input uncertainty may exist, only a subset of these sources may impact the uncertainty in the calculated output, SD(C). Several sources of uncertainty can be eliminated from the final UQ analysis by sensitivity studies. These studies quantify reduced chi-squared values by comparing models with input perturbations that represent bounding extremes for a given model input parameter. If the reduced chi-squared value is small for the minimum or maximum perturbation cases, the input uncertainty is insignificant. It is important to note that this procedure is dependent on the experimental measurement uncertainties, so it is tied not only to this particular sample and calculation methodology but also to the measurement laboratory. Therefore any modeling-based conclusions may differ for another similar sample and are not necessarily general. Only the RCA sample at the 13.20 cm axial location (27.35 GWd/MTU EOL burnup) is utilized to assess the significance of modeling decisions or input data on calculation bias.

2.2. Modeling-based Bias Assessment Analysis

2.2.1. Self-Shielding Treatment

The first modeling decision analyzed in this work is the selection of the self-shielding method in SCALE, i.e., the BONAMI-based (full Bondarenko treatment) or CENTRM-based (explicit slowing-down) self-shielding method. The CENTRM-based method is more accurate and more rigorous, i.e., higher-fidelity, but at the cost of significantly longer run times when compared to BONAMI-based calculations. In order to compare the impact of the selection of the self-shielding method on isotopic predictions, isotopic predictions have been compared for a CENTRM-based calculation and a BONAMI-based calculation. The bias introduced by utilizing the BONAMI-based method has been determined to be significant, with a reduced-chi-squared value of 0.513. However, due to reduced run-time requirements, the BONAMI-based method is employed in the input-based uncertainty analysis. A bias factor correction is employed in the uncertainty analysis.

2.2.2. Fuel Temperature Distribution

The second modeling decision investigated is the within-pin fuel temperature distribution. The effect of radial temperature profiles on isotopic predictions has been previously studied using SCALE [7]. The results from K. Clarno et al. show that modeling the radial temperature profile of a fuel rod with 10 rings can improve accuracy in EOL isotopic concentrations by as much as a percent for certain isotopes when compared to an effective fuel temperature model. Although these disagreements may seem negligible, they may be significant when compared to the measurement uncertainty of certain isotopes (2.3% for major actinides). In this work, two CENTRM-based models have been developed: one with an effective fuel temperature and the other with a 20-ring radial temperature profile. The effective fuel temperature model introduces a significant bias (reduced-chi-squared of 0.289), confirming the results of [7], but due to run-time limitations, the effective fuel temperature model is utilized in the uncertainty analysis. A bias factor correction for the temperature distribution is also employed in the uncertainty analysis.

2.2.3. Nuclide Tracking Set

The next modeling decision investigated in this study is the use of a truncated nuclide tracking set in SCALE, which is controlled by the *addnux* parameter [1]. The nuclide tracking set to use in this analysis tracks 94 isotopes in each depletion material in the SCALE transport model. Utilizing this simplified tracking set over the other more-comprehensive options introduces a negligible bias (reduced-chi-squared of 0.053) in isotopic predictions. The use of this set also considerably reduces SCALE run-times, which further justifies its use.

2.3. Input-based Bias Assessment Analysis

2.3.1. Power History

The first input parameter assessed is the power history (or operating history) of the CC-1 reactor.

Uncertainties for the power histories of each sample (axial location) at each time interval are not provided for CC-1. A strategy has been developed in order to incorporate some uncertainty of the power history by representing the specific power history for a particular cycle and axial location, $P(z, \Delta t)$, as a product of four factors:

$$P(z, \Delta t) = f_{shape}(z, \Delta t)\, \bar{f}_{Rod}\, \bar{f}_{Asm}\, \bar{P}_{Core} \ ,$$

where $\bar{P}_{Core}$ is the average specific power (W/g) of the core for the cycle, and $\bar{f}_{Rod}$ and $\bar{f}_{Asm}$ are the rod and assembly power factors for that particular cycle and are defined as the ratio of the rod cycle-averaged burnup to the assembly cycle-averaged burnup and as the ratio of the assembly cycle-averaged burnup to core cycle-averaged burnup, respectively. $\bar{P}_{Core}$, $\bar{f}_{Rod}$, and $\bar{f}_{Asm}$ are computed from provided data for CC-1. Lastly, $f_{shape}(z, \Delta t)$ is defined as the axial shape function of the specific power history and is determined by solving the above equation at every time interval and at every axial location.

As expected, the rod and assembly power factors introduce significant uncertainties to SCALE isotopic predictions and are included in the uncertainty analysis of assembly D047. The uncertainty in the rod power factor was conservatively estimated to be 2.0% for each cycle, based on the observation that the pin powers vary less than 5% across the assembly. The uncertainty in the average assembly power has been shown to be largely dependent on its location in the core [8]. Comparing the location of the D047 assembly to the results shown by M. Klein et al. allows the uncertainty in the assembly power factor to be approximated to be 3% and 5% for cycles 2 and 5, respectively, and 2% for cycles 3 and 4. The uncertainties of the powers reported in Appendix A have been determined by propagating the uncertainties of the rod and assembly power factors for the 13.20 cm axial location. SCALE isotopic results were also very sensitive to perturbations in the axial power shape function, but a realistic time-varying shape was deemed too complex to include in this analysis and was consequently not included in the final Sampler model. No uncertainty data are provided in the literature for the cycle-averaged core specific power, and its uncertainty is assumed to be negligible.

For this work, the power history of each axial location was normalized to each location's respective measured EOL burnup. However, calculations were also performed without normalizing the power history for the highest-burnup case for comparison purposes, shown in Appendix B. In future work, the assembly power history will be a calculated quantity, i.e., calculated by a core simulator, and the uncertainty will no longer need to be supplied in the literature and instead can be approximated from the core simulation. Data assimilation will then be used to adjust all uncertain/biased input, including the given core power history and calculated power factors. In this type of analysis, the burnup bias will be a key parameter to evaluate the corrections.

2.3.2. Other Uncertainties

Uncertainty information is provided for both the uranium weight percent (γ_U) and the fuel material density ($\rho_{UO_2,mat}$) [9]. However, it was observed that when the amount of uranium present in the fuel rod was preserved, SCALE isotopic predictions are largely insensitive to perturbations to these parameters.

Another input uncertainty that was considered in this study is the uncertainty in the fuel cladding

thickness. Assuming a fixed inner diameter, perturbing the cladding thickness displaces the moderator, which significantly affects the accuracy of the predictions of several reactor physics parameters. Since no uncertainty information is available, the relative uncertainty of the cladding thickness was approximated as 3.7% [10]. SCALE isotopic predictions have been found to be sensitive to perturbations to the cladding thickness, and thus this uncertainty is incorporated into the final uncertainty analysis.

The last input parameter uncertainty considered is the uncertainty for the soluble boron concentration history provided in the CC-1 literature, which was found to have an insignificant effect on SCALE isotopic predictions (reduced chi-squared of 0.0812) and not included in the uncertainty analysis. For large perturbations of ±50 ppm of the entire soluble boron history, the relative differences between the perturbed cases and the nominal case were 9.7% and 20.4% of a measurement SD for U-235 and Pu-239, respectively.

A potentially important bias effect due to the assembly leakage, which is space and time dependent, was not assessed. The sample location is an interior rod, and so this is not expected to have a large impact. The moderator density is another component that was left out, due to its unknown correlation with the assembly and rod powers. Future work with a core simulator will investigate these effects.

2.4. Final Sampler Model for Uncertainty Analysis

The modeling-based and input-based bias assessment investigations performed in this work are summarized in Table 2 and Table 3, respectively. The "Magnitude" column in Table 3 specifies the range of variation or the uncertainty utilized for that particular parameter with the "Variation" column providing some other pertinent information. Tables 2 and 3 also display the RMS metric used to determine the significance of each modeling decision or input parameter, i.e., the square root of the reduced chi-squared of the comparison.

Table 2. Summary of modeling-based bias assessment studies performed.

Modeling Decision	Description	RMS	Decision
Self-Shielding Treatment	BONAMI vs. CENTRM	0.516	BONAMI*
Radial Temperature Profile	T_{eff} vs. 20 rings	0.289	T_{eff}*
Nuclide Tracking Set	94 vs. 245 vs. 403 nuclides	0.053	94†

*chosen due to run-time limitations; introduces a significant bias.
† chosen due to run-time limitations; does not introduce a significant bias.

Table 3. Summary of input-uncertainty studies performed.

Input Parameter	Variation	Magnitude	RMS	Decision
Pellet Density	Uniform Dist.	$10.36 - 10.48$ g/cm^3	0.018	Not Included
Uranium wt. %	Normal Dist.	0.03%		Not Included
Shape Function	Min/Max Sensitivity	10% Peaking/Flattening	4.89	Not Included
Rod Power Factor	Uniform Dist.	2.0%	0.255	Included
Assembly Power Factor	Normal Dist.	Varies with position	0.707	Included
Soluble Boron	Min/Max Sensitivity	± 50 ppm	0.081	Not Included
Cladding Thickness	Min/Max Sensitivity	± 3.72%	0.195	Included

3. RESULTS

The assembly model is analyzed using SCALE Sampler for each axial location with input uncertainties for the cladding thickness, rod and assembly power factors, multigroup cross sections, decay constants, and fission product yields. As summarized in Table 2, the SCALE Sampler model utilized Bondarenko-based self-shielding (BONAMI module), an effective fuel temperature model, and 94 nuclides tracked in each depletion material in the SCALE transport model. All isotopic results from the nominal (unperturbed) calculation at each axial location were converted to g/g $U_{initial}$ to compare to measurements reported in the literature for CC-1. Each axial location is modeled thrice in Sampler: once with all nuclear data uncertainty (cross sections, decay constants, and fission product yields), once with only input parameter uncertainty, and one with all considered nuclear data and input uncertainties. Each of these cases had their nominal values perturbed 100 times by Sampler and all perturbation calculations were performed in parallel.

From the Sampler output of each axial location, relative standard deviations (RSDs) are available for the predicted isotopic concentrations. The calculated isotopic prediction uncertainties for each axial location are displayed in Figures 2 and 3, which consider only uncertainties in input parameters and nuclear data, respectively. The isotopic predictions of the nominal case were then compared to the actual isotopic measurements by calculating the C/E ratios for each isotope of each axial sample where the uncertainty of the C/E value was determined by propagating the uncertainty from the isotopic measurements and the uncertainty in SCALE isotopic predictions. The isotopes with C/E-1 less than 20% are shown in Figure 4, while all other isotopes are presented in Figure 5. Error bars are shown in both figures and correspond to a single SD. Further, the isotopic prediction biases for the high-burnup case while utilizing a normalized and non-normalized power history are shown in Figure 6. The C/E-1 values and their respective uncertainties displayed in Figure 6 are shown in Appendix B.

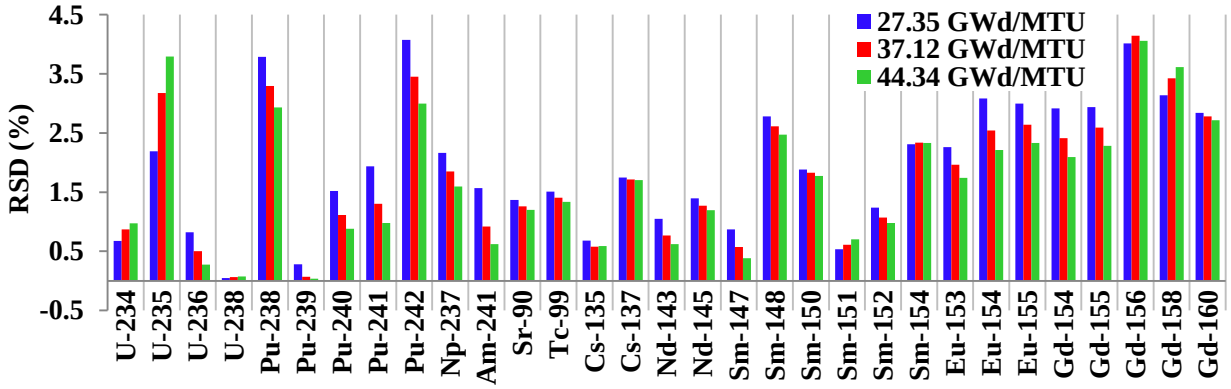

Figure 2. Isotopic uncertainty due to input parameter uncertainty.

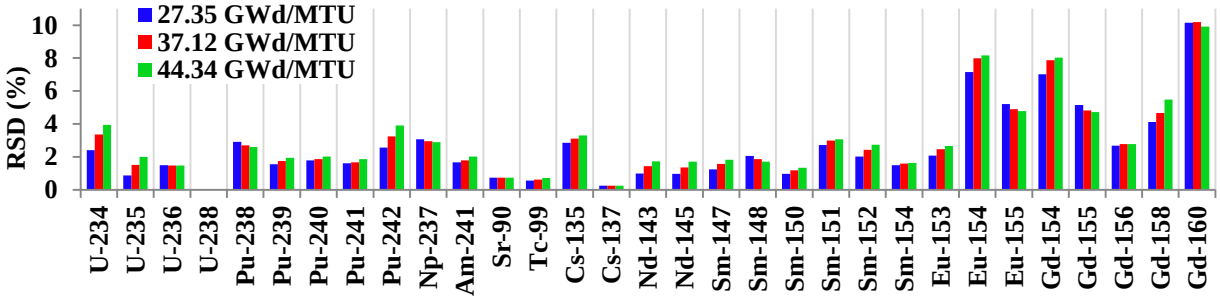

Figure 3. Isotopic uncertainty due to nuclear data uncertainty.

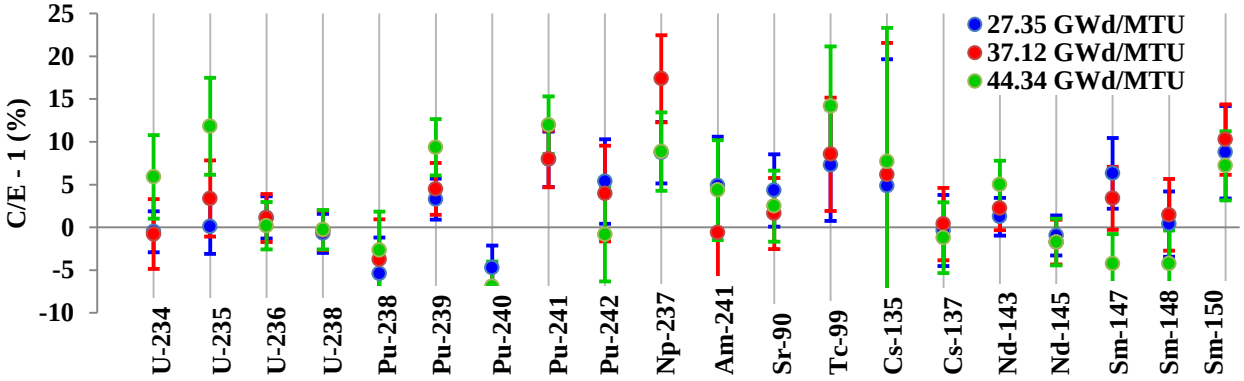

Figure 4. Biases not exceeding 20% with 1-sigma error bars for each axial location.

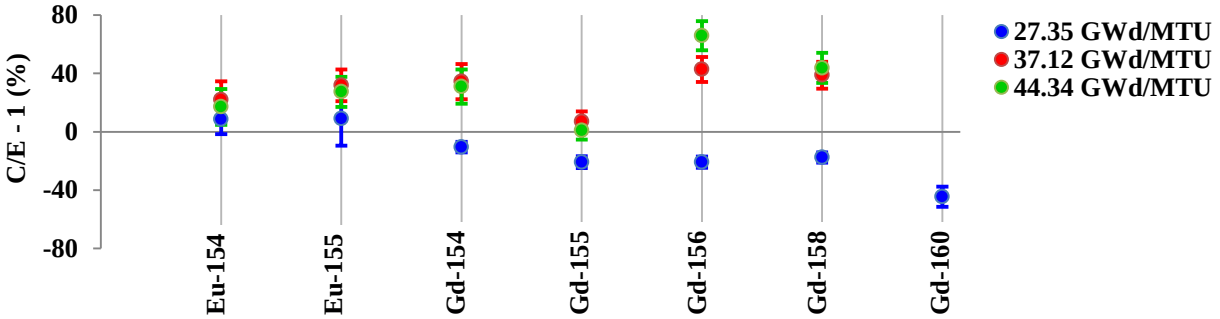

Figure 5. Biases exceeding 20% with 1-sigma error bars for each axial location.

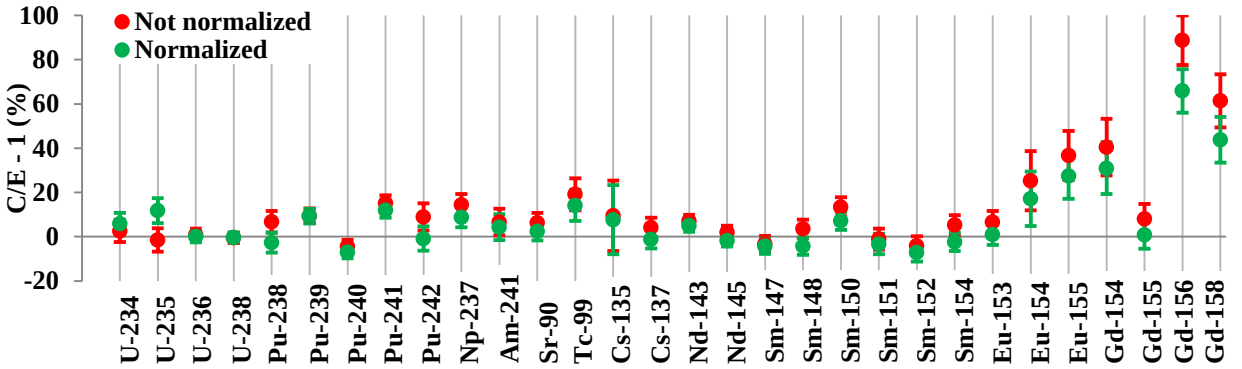

Figure 6. Biases for the 44.34 GWd/MTU case with and without power history normalization.

3.1. Analysis

In terms of isotopic depletion, the effect of uncertain inputs (i.e., everything but nuclear data, as shown in Figure 2) induce flux spectrum uncertainty which affects the uranium depletion, plutonium production/depletion, and fission product build-up. In Figure 3, the effect of uncertain nuclear data is shown, which has the potential to affect the isotopic reaction rates directly and indirectly through flux spectrum changes. However, all in all, the *relative* uncertainty in a particular isotope as a function of burnup varies only slightly from 27.35 to 44.34 GWd/MTU in both cases. The following observations are made from Figures 2 and 3.

- The U-235 uncertainty is greater for input than nuclear data, but even at the lowest burnup, there is little U-235 remaining in the fuel and Pu-239 fission is dominating.
- The Pu-239 uncertainty shows the opposite: the uncertainty caused by uncertain input is extremely small, most likely due to the small changes in production from U-238 resulting from an uncertain flux spectrum, while the Pu-239 uncertainty due to nuclear data is on par with other minor actinides at 2-3%.
- The Eu and Gd isotopes generally show large (>5%) uncertainty from nuclear data.

From the bias plus uncertainty shown in Figure 4, for many isotopes, similar biases/uncertainties exist for the lower burnup samples (27.35 and 37.12 GWd/MTU), whereas the highest 44.34 GWd/MTU sample shows a different result, sometimes with a different sign. The largest discrepancies can be seen in Figure 5 and occur for the isotopic predictions of the even-numbered gadolinium isotopes. For these isotopes, one can observe a significant underprediction for the lowest burnup case and significant overpredictions for the two higher burnup cases. These significant discrepancies can be attributed to: (i) biases present in the operating history for CC-1; (ii) biases in the multigroup nuclear data for the gadolinium isotopes; (iii) modeling biases; or (iv) measurement biases far outside the reported measurement uncertainty. The operating history uncertainty has been sufficiently approximated such that (i) seems unlikely to account for such large biases in stable isotopes. Future cross-section sensitivity work will investigate (ii) and (iii) and if insufficient sensitivity is found, process of elimination would suggest a significant bias in the measurements for the even-numbered gadolinia isotopes: Gd-154, Gd-156, and Gd-158. Figure 6 shows the effect of normalizing the power history to match the EOL burnup for the highest burnup case. With normalization, the biases in isotopic predictions are observed to decrease. This is expected due to the strong relationship between isotopic predictions and fuel burnup.

The significance of the biases shown in Figures 4 and 5 of each isotopic prediction may be analyzed by calculating the magnitude of the bias in terms of number of standard deviations (SDs).

A bias greater than two SDs is most likely significant due to the small probability that the bias will lie outside two SDs from its expected value. Biases between one and two SDs may or may not be significant, and further analysis of the cause of the bias is warranted. Isotopes with significant biases for any case, i.e., bias greater than 2 SDs, are listed in Table 4 along with the magnitude of the bias in terms of the bias SD. Biases are not available for Gd-160 for all axial locations due to a lack of measurement data.

Table 4. Isotopes with significant biases (shown as number of SDs) in isotopic predictions.

Isotope	EOL Burnup (GWd/MTU)		
	27.35	**37.12**	**44.34**
Pu-239	1.4	1.5	2.8
Pu-240	-1.8	-2.6	-2.4
Pu-241	2.5	2.4	3.5
Np-237	2.4	3.4	1.9
Sm-154	-1.3	2.7	-0.6
Eu-153	2.4	0.9	0.2
Eu-155	0.5	2.9	2.7
Gd-154	-2.9	2.9	2.6
Gd-155	-5.1	1.0	0.1
Gd-156	-5.5	5.0	6.7
Gd-158	-5.1	4.2	4.2
Gd-160	-6.5	N/A	N/A

4. CONCLUSIONS

Significant biases have been identified in EOL isotopic predictions for certain plutonium and gadolinium isotopes at all axial locations. In this context, *significant* means that the bias distribution does not include C/E-1=0 as a probable value, where the distribution/uncertainty in the bias has been determined from uncertainty in measurement E *and* in calculation C. In the past, the uncertainty in calculation C has been neglected. New tools such as SCALE Sampler allow it's calculation with rigorous propagation of uncertainty. The next stage is to investigate the sources of the significant biases, e.g., in the literature-provided data for CC-1 and in the nuclear data utilized in this study from ENDF/B-VII.0 nuclear data files. Furthermore, nuclear data uncertainties have been observed to have a significant effect on the isotopic predictions of Eu-154, Gd-154, and Gd-160 and an investigation into the sources of these effects is warranted. The observed isotopic prediction uncertainty resulting from perturbations to the CC-1 power history is found to be significant, although it should be noted that the power uncertainty does not correspond to the actual uncertainty of the power given in the benchmark, but is estimated from various sources. The calculation of true power uncertainty requires full-core simulation with Sampler, as well as knowledge of the loading pattern for each cycle and all assembly design details, which is not provided in the CC-1 data set. Future work will look at other RCA data sets with enough charac-

terization to permit full core simulation with Sampler and proper incorporation of power uncertainties. These investigations are left as future work for this study as well as the objectives to extend the list of considered isotopes and input parameter uncertainties for the input-based bias assessment.

ACKNOWLEDGMENTS

This work has been partially funded by both Oak Ridge National Laboratory (ORNL) and the Nuclear Regulatory Commission. This research was performed during the Nuclear Engineering Science Laboratory Synthesis (NESLS) program of ORNL.

REFERENCES

[1] *SCALE: A Modular Code System for Performing Standardized Computer Analyses for Licensing Evaluations*, ORNL/TM-2005/39, Version 6.1, Oak Ridge National Laboratory, Oak Ridge, Tenn., June 2011.

[2] M. L. Williams, G. Ilas, M. A. Jessee, B. T. Rearden, D. Wiarda, W. Zwermann, L. Gallner, M. Klein, B. Krzykacz-Hausmann, and A. Pautz, "A Statistical Sampling Method for Uncertainty Analysis with SCALE and XSUSA," *Nuclear Technology* 2013, 183, pp. 515-526.

[3] M. D. DeHart and S. M. Bowman, "Reactor Physics Methods and Analysis Capabilities in SCALE," *Nuclear Technology* 2011, 174, pp. 196-213.

[4] R. J. Guenther, D. E. Blahnik, U. P. Jenquin, J. E. Mendel, L. E. Thomas, and C. K. Thornhill, *Characterization of Spent Fuel Approved Testing Material—ATM-104*, Pacific Northwest Laboratory, PNL-5109-104 (UC-802), December 1991.

[5] G. Radulescu, I. C. Gauld, and G. Ilas, *SCALE 5.1 Predictions of PWR Spent Nuclear Fuel Isotopic Compositions*, ORNL/TM-2010/44, Oak Ridge National Laboratory, Oak Ridge, Tenn., March 2010.

[6] Y. Ronen, *Uncertainty Analysis*, CRC Press, 1988.

[7] T. Greifenkamp, K. T. Clarno, and J. C. Gehin, "Effect of Fuel Temperature Profile on Eigenvalue Calculations," Proceedings of the 2008 American Nuclear Society Student Conference, Texas A&M University, February 2008.

[8] M. Klein, M. Bock, L. Gallner, B. Krzykacz-Hausmann, A. Pautz, K. Velkov, and W. Zwermann. (May 2012). GRS results for Phase I. *UAM-7*. Lecture conducted from Karlsruhe Institute of Technology, Karlsruhe, Germany.

[9] S. R. Bierman, *Spent Reactor Fuel Benchmark Composition Data for Code Validation*, Pacific Northwest Laboratory, Richland, Washington, September 1991.

[10] K. Ivanov, M. Avramova, S. Kamerow, I. Kodeli, E. Sartori, E. Ivanov, and O. Cabellos, *Benchmark for Uncertainty Analysis in Modelling (UAM) for the Design, Operation and Safety Analysis of LWRs*, NEA/NSC/DOC(2013)7, May, 2013.

APPENDIX A. ISOTOPIC MEASUREMENTS AND POWER HISTORY FOR CC-1

Table A-1. PNNL isotopic measurement data for fuel rod MKP109 axial samples [5].

Isotope	27.35 GWd/MTU		37.12 GWd/MTU		44.34 GWd/MTU	
	g/g $U_{initial}$	RSD (%)*	g/g $U_{initial}$	RSD (%)*	g/g $U_{initial}$	RSD (%)*
U-234	1.82E-04	2.3	1.59E-04	2.3	1.36E-04	2.3
U-235	9.61E-03	2.3	5.87E-03	2.3	4.02E-03	2.3
U-236	3.56E-03	2.3	4.00E-03	2.3	4.19E-03	2.3
U-238	9.56E-01	2.3	9.45E-01	2.3	9.36E-01	2.3
Pu-238	1.15E-04	2.3	2.14E-04	2.3	3.05E-04	2.3
Pu-239	4.83E-03	2.3	4.95E-03	2.3	4.95E-03	2.3
Pu-240	1.95E-03	2.3	2.54E-03	2.3	2.88E-03	2.3
Pu-241	7.73E-04	2.3	1.02E-03	2.3	1.16E-03	2.3
Pu-242	3.28E-04	2.3	6.53E-04	2.3	9.53E-04	2.3
Np-237	3.04E-04	2.5	4.04E-04	2.5	5.31E-04	2.5
Am-241	2.82E-04	5.2	3.89E-04	5.2	4.32E-04	5.2
Sr-90	3.78E-04	3.8	4.86E-04	3.8	5.41E-04	3.8
Tc-99	6.35E-04	5.9	8.17E-04	5.9	8.85E-04	5.9
Cs-135	4.08E-04	14.1	4.54E-04	14.1	4.88E-04	14.1
Cs-137	8.74E-04	3.8	1.18E-03	3.8	1.42E-03	3.8
Nd-143	6.95E-04	1.9	8.12E-04	1.9	8.66E-04	1.9
Nd-145	5.79E-04	1.9	7.41E-04	1.9	8.44E-04	1.9

*Measurement RSDs are utilized to quantify significance in input uncertainty and bias assessments.

Table A-2. KRI isotopic measurement data for fuel rod MKP109 axial samples [5].

Isotope	27.35 GWd/MTU		37.12 GWd/MTU		44.34 GWd/MTU	
	g/g $U_{initial}$	RSD (%)*	g/g $U_{initial}$	RSD (%)*	g/g $U_{initial}$	RSD (%)*
Sm-147	2.30E-04	3.8	2.70E-04	3.1	3.08E-04	3.8
Sm-148	1.00E-04	2.6	1.61E-04	3.0	2.24E-04	3.8
Sm-150	2.09E-04	4.6	2.90E-04	3.0	3.64E-04	3.8
Sm-151	7.53E-06	38.5	9.41E-06	3.7	1.07E-05	5.1
Sm-152	8.97E-05	3.7	1.10E-04	3.3	1.33E-04	4.3
Sm-154	3.07E-05	6.0	3.81E-05	3.0	5.63E-05	3.8
Eu-153	8.52E-05	2.6	1.30E-04	3.3	1.62E-04	3.4
Eu-154	6.08E-06	8.8	8.76E-06	6.4	1.09E-05	7.0
Eu-155	1.04E-06	16.8	1.37E-06	6.2	1.79E-06	6.9
Gd-154	1.37E-05	2.8	1.50E-05	3.6	2.00E-05	3.9
Gd-155	6.25E-06	4.2	7.41E-06	3.6	9.96E-06	3.9
Gd-156	6.37E-05	2.6	7.33E-05	3.6	9.51E-05	3.9
Gd-158	1.40E-05	2.8	1.49E-05	3.6	2.06E-05	3.9
Gd-160	1.45E-06	12.1	-	-	-	-

*Measurement RSDs are utilized to quantify significance in input uncertainty and bias assessments.

Table A-3. Power history for 13.20 cm axial location [5].

	Interval (days)	LHGR (kW/m)	RSD (%)		Interval (days)	LHGR (kW/m)	RSD (%)
Cycle 2	7.0	6.56	3.606	**Cycle 3**	7.9	8.63	2.828
	30.8	8.96	3.606		14.4	8.89	2.828
	16.3	9.19	3.606		19.7	7.02	2.828
	11.4	9.38	3.606		16.8	10.43	2.828
	12.5	9.65	3.606		16.3	10.99	2.828
	23.7	9.88	3.606		15.4	12.27	2.828
	22.8	10.37	3.606		39.1	12.17	2.828
	23.2	10.73	3.606		31.2	12.96	2.828
	8.1	10.83	3.606		31.8	13.39	2.828
	31.4	11.42	3.606		31.8	13.78	2.828
	34.3	11.78	3.606		44.3	14.37	2.828
	16.4	12.30	3.606		25.0	0.00	2.828
	19.2	12.30	3.606		59.1	15.32	2.828
	12.8	12.50	3.606		28.9	16.24	2.828
	34.2	11.91	3.606		*81.0*	0.00	0.000
	1.9	11.94	3.606				
	71.0	0.00	0.000				

	Interval (days)	LHGR (kW/m)	RSD (%)		Interval (days)	LHGR (kW/m)	RSD (%)
Cycle 4	46.1	9.15	2.828	**Cycle 5**	65.0	6.50	5.385
	24.0	9.55	2.828		5.5	7.05	5.385
	22.6	10.07	2.828		6.6	7.22	5.385
	25.7	10.79	2.828		28.6	7.74	5.385
	30.2	5.15	2.828		31.2	8.33	5.385
	41.2	5.87	2.828		27.0	8.73	5.385
	50.3	5.64	2.828		22.7	9.09	5.385
	11.0	10.43	2.828		27.1	8.07	5.385
	32.8	12.89	2.828		55.2	9.22	5.385
	23.5	13.35	2.828		20.9	10.40	5.385
	29.4	13.29	2.828		41.9	10.89	5.385
	28.1	13.94	2.828		21.6	11.09	5.385
	65.4	14.50	2.828		27.6	10.53	5.385
	35.7	15.16	2.828		19.0	11.71	5.385
	85.0	0.00	0.000		61.2	10.01	5.385
					Cooling time	0.00	0.00

APPENDIX B. ISOTOPIC PREDICTION BIASES WITH AND WITHOUT NORMALIZATION TO MEASURED BURNUP

Table B-1. C/E-1 values and uncertainties for the 165.22 cm axial location case with and without the power history normalized to the measured EOL burnup (44.34 GWd/MTU).

Isotope	165.22 cm axial location			
	Not normalized		Normalized	
	C/E-1 (%)	SD (%)	C/E-1 (%)	SD (%)
U-234	2.64	4.97	5.90	4.89
U-235	-1.43	5.30	11.82	5.67
U-236	0.92	2.77	0.19	2.77
U-238	-0.47	2.29	-0.28	2.29
Pu-238	6.75	4.83	-2.65	4.48
Pu-239	9.44	3.33	9.35	3.29
Pu-240	-4.32	2.98	-6.90	2.91
Pu-241	15.21	3.50	11.95	3.38
Pu-242	8.99	6.15	-0.84	5.49
Np-237	14.47	4.80	8.87	4.58
Am-241	6.63	5.99	4.35	5.84
Sr-90	6.39	4.32	2.48	4.17
Tc-99	19.18	7.27	14.18	6.97
Cs-135	9.51	15.90	7.71	15.61
Cs-137	4.24	4.37	-1.20	4.14
Nd-143	7.03	2.92	4.99	2.80
Nd-145	2.09	2.91	-1.72	2.74
Sm-147	-3.18	3.56	-4.26	3.49
Sm-148	3.57	4.15	-4.25	3.87
Sm-150	13.51	4.31	7.20	4.05
Sm-151	-1.05	4.80	-3.28	4.67
Sm-152	-4.05	4.31	-7.08	4.13
Sm-154	5.30	4.45	-2.29	4.11
Eu-153	6.70	4.95	0.95	4.67
Eu-154	25.29	13.34	17.14	12.29
Eu-155	36.73	11.01	27.44	10.34
Gd-154	40.44	12.81	31.01	11.73
Gd-155	8.16	6.72	0.93	6.36
Gd-156	88.76	11.21	65.89	9.90
Gd-158	61.41	12.05	43.78	10.35